JOURNAL OF PHYSICAL ORGANIC CHEMISTRY
J. Phys. Org. Chem. 2004; **17:** 777–786
Published online in Wiley InterScience (www.interscience.wiley.com). DOI: 10.1002/poc.794

Structure and reactions of the peroxy radicals of glycine and alanine in peptides: an *ab initio* study†

Mei Lan Huang‡ **and Arvi Rauk***

Department of Chemistry, University of Calgary, 2500 University Drive, Calgary, Alberta, T2N 1N4 Canada

epoc

ABSTRACT: *Ab initio* calculations at the B3LYP/6-31G(d) and CBS-RAD level were carried out to investigate the reaction of $^{\alpha}$C-centered peroxy radicals of neutral, non-zwitterionic glycine and alanine (AH), and as residues in model peptides, *N*-formylglycinamide and *N*-formylalaninamide (PH). Bond dissociation enthalpies (BDEs) were calculated for the $^{\alpha}$C—O (D^{α}_{CO}), O—O (D_{OO}) and O—H (D_{OH}) bonds of glycine and alanine peroxy radicals (AOO, POO) and hydroperoxides (AOOH, POOH). The predicted BDEs at 298 K, in kJ mol^{-1} are AOO(Gly), $D^{\alpha}_{CO} = 70$; AOO(Ala), $D^{\alpha}_{CO} = 69$; POO(Gly), $D^{\alpha}_{CO} = 89$; POO(Ala), $D^{\alpha}_{CO} = 86$; AOOH(Gly), $D^{\alpha}_{CO} = 237$, $D_{OO} = 203$, $D_{OH} = 371$; AOOH(Ala), $D^{\alpha}_{CO} = 234$, $D_{OO} = 195$, $D_{OH} = 368$; POOH(Gly), $D^{\alpha}_{OH} = 266$, $D_{OO} = 207$, $D_{OH} = 380$; POOH(Ala), $D^{\alpha}_{CO} = 264$, $D_{OO} = 208$, $D_{OH} = 383$. Values of BDE of the peptides in β-sheet peptide conformations were also estimated by constraining the Ramachandran dihedral angles, Φ and Ψ to, values of $-150°$ and $+150°$: (*S*)-POO(Gly), $D^{\alpha}_{CO} = 99$; (*R*)-POO(Gly), $D^{\alpha}_{CO} = 78$; (*S*)-POO(Ala), $D^{\alpha}_{CO} = 88$; (*R*)-POO(Ala), $D^{\alpha}_{CO} = 83$; (*S*)-POOH(Gly), $D^{\alpha}_{CO} = 258$, $D_{OO} = 195$, $D_{OH} = 362$; (*R*)-POOH(Gly), $D^{\alpha}_{CO} = 278$, $D_{OO} = 217$, $D_{OH} = 404$; (*S*)-POOH(Ala), $D^{\alpha}_{CO} = 240$, $D_{OO} = 192$, $D_{OH} = 355$; (*R*)-POOH(Ala), $D^{\alpha}_{CO} = 270$, $D_{OO} = 204$, $D_{OH} = 390$. The reactions of $^{\alpha}$C-peroxy radicals, POO, and $^{\alpha}$C-alkoxy radicals, PO, were studied in detail.

Additional material for this paper is available in Wiley Interscience

KEYWORDS: *ab initio*; peptide; oxidation; bond dissociation energies; isodesmic reaction; peroxy radical; peroxyl radical

INTRODUCTION

Oxidation of proteins has been suggested to be the cause of pathological disorders, such as protein turnover, cataractgenesis, atherosclerosis and tissue injury during ischemia–reperfusion.[1] The generation and propagation reactions of radicals of proteins has been reviewed by Hawkins and Davies.[2] Reactive oxidative species (ROS) produced by toxic chemicals or radiation, or by detoxification of extraneous chemicals in the liver[3–5] may generate radicals in the side-chains and backbone of amino acid residues. We are primarily concerned here with the captodatively stabilized $^{\alpha}$C-centered radicals, $^{\alpha}$P$^{\cdot}$, on the peptide backbone. Particularly in the oxygen-enriched interiors of lipid bilayers, these can add O_2 to produce more reactive peroxyl radicals, POO, and initiate lipid oxidation. Lipid oxidation has been proposed to be especially damaging, because it is self-propagating and because the brain is relatively enriched in polyunsaturated fatty acids, the prime substrates for lipid peroxidation. Accumulation of lipid peroxidation products can be found in diseased regions of Alzheimer's diseased brains.[6–8]

Because of their importance, the reactions of peptide-derived peroxy radicals and hydroperoxides have been extensively studied experimentally[3,9–13] and, to a lesser extent, by computational means. The results of these investigations are discussed below in connection with the present study.

The terminology used in this paper is consistent with that introduced previously.[14] The model peptide units, *N*-formylglycinamide and *N*-formylalaninamide (a model for most other residues), are designated PH(Gly) and PH(Ala), respectively, or simply PH. The corresponding $^{\alpha}$C-centered radicals are designated $^{\alpha}$P$^{\cdot}$, and the derivative hydroperoxides, peroxy radicals and alkoxy radicals as POOH, POO and PO, respectively. In a consistent manner, the neutral amino acid $^{\alpha}$C-hydroperoxides and their radical counterparts are designated AOOH, AOO and AO.

The proposed reactions of peroxy radicals[9] examined in the present study are illustrated in Scheme 1. The $^{\alpha}$C-centered radicals can trap molecular oxygen to form a peroxy radical (step 2). The peroxy radicals undergo a complex series of reactions: loss of O_2 to recover $^{\alpha}$C-centered radical (step −2); H-atom abstraction from lipids or other H donors (such as SH, CH_2 or $^{\alpha}$CH of the peptide) to give rise to a $^{\alpha}$C-hydroperoxide (step 3); elimination of $HO_2^{\cdot}$ in a concerted fashion (step 4), or

**Correspondence to:* A. Rauk, Department of Chemistry, University of Calgary, 2500 University Drive, Calgary, Alberta, T2N 1N4 Canada.
E-mail: rauk@ucalgary.ca
Contract/grant sponsor: Natural Sciences and Engineering Council of Canada (NSERC).
†In honour of Kurt Mislow.
‡Present address: Department of Chemistry, Central Chemistry Laboratory, South Parks Road, Oxford OX1 3QH, UK.

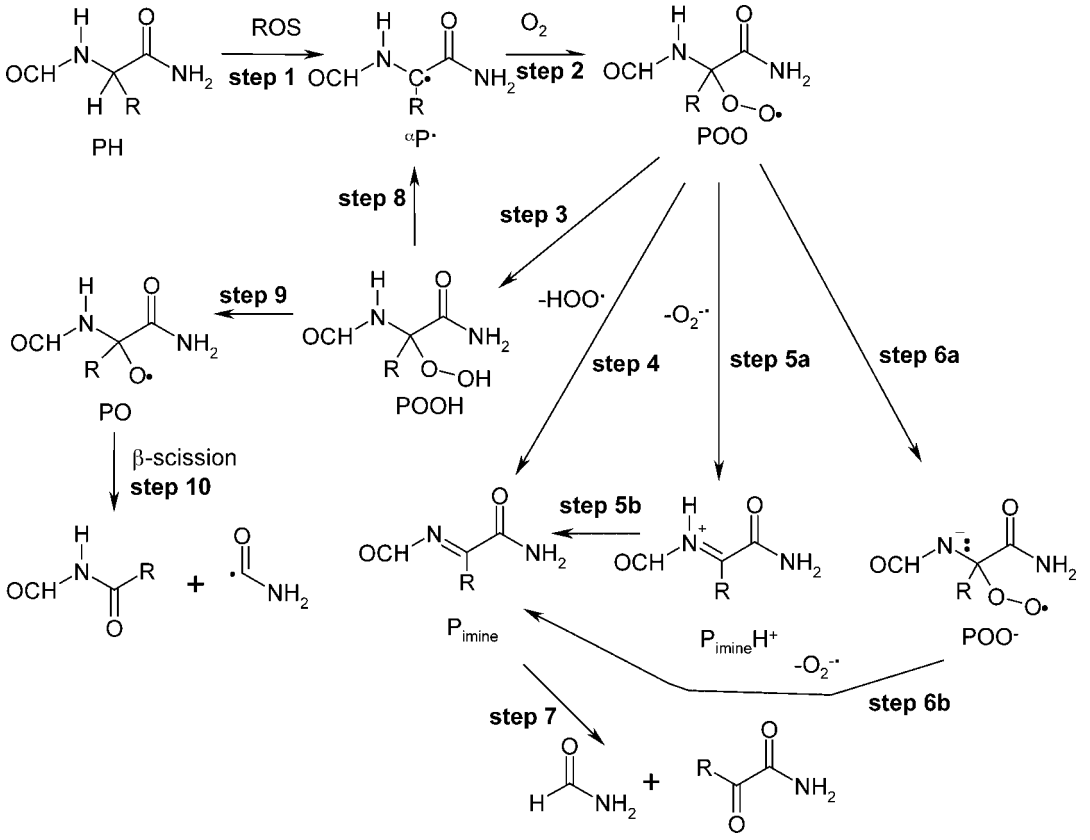

Scheme 1. Reactions involving peroxy radicals discussed in the text

stepwise by heterolysis (steps 5a and b) or under base catalysis (steps 6a and b). The end products of steps 4–6 are acylimines that subsequently break the backbone $^{\alpha}$C—N bond by hydrolyis to form amides and bicarbonyl compounds (step 7). The hydroperoxides from step 3 can potentially lose $HO_2^{\bullet}$, reforming $^{\alpha}$C-centered radicals (step 8), or undergo thermolysis or reductive cleavage of the O—O bond to give $^{\alpha}$C-alkoxy radicals (step 9)[15,16] that in turn can undergo various β-scission reactions to yield carbonyl groups and acyl radicals (e.g. step 10).

COMPUTATIONAL METHODS

All *ab initio* calculations were performed with the Gaussian 98 suite of programs.[17] The geometry optimization and frequency calculations were carried out initially at the B3LYP/6–31G(d) level. The vibrational frequencies were scaled by a factor of 0.9806 in considering the zero-point energy. Three different initial positions of the O—O bond relative to the $^{\alpha}$C—N and $^{\alpha}$C—$^{\text{carboxyl}}$C bonds were considered for hydroperoxides and also for the peroxy radicals. The optimized structure with minimum energy was selected for higher level calculations, namely geometry optimization or single-point energy evaluation at the B3LYP/6–311+G(3df,2p) level. CBS-RAD energy calculation[18] was carried out to estimate differences of enthalpies of reaction for all glycine-derived species. The CBS-RAD procedure is designed to give reliable thermochemical results for free radicals.[18] Bond dissociation enthalpies (BDEs) of alanine-derived species and all geometry-constrained species were derived from isodesmic reactions as described below.

In the case of heterolytic dissociation and base-catalyzed elimination involving superoxide anion radical ($O_2^{-\cdot}$), free energies of solvation for reactions were estimated using the polarized conductor model (CPCM)[19] as implemented in Gaussian 98. For each species in the CPCM calculation, radii for atom-centered spheres were chosen to match the 0.001 electron bohr^{-3} isodensity surface.

Bond dissociation enthalpies (BDEs)

The B3LYP/6–31G(d) procedure was shown by Armstrong *et al.* to give reliable results for the $^{\alpha}$C—H BDE of neutral amino acids, AH and amino acid residues in peptides, PH, when used in combination with an isodesmic correction.[20] This procedure is also expected to yield accurate BDEs of $^{\alpha}$C—O, O—O and O—H bonds when used with a suitable isodesmic partner. The $^{\alpha}$C—O BDEs of peroxy radical, $D_{\alpha CO}$, are defined as the heat of reaction (1), $\Delta H°(1)$.

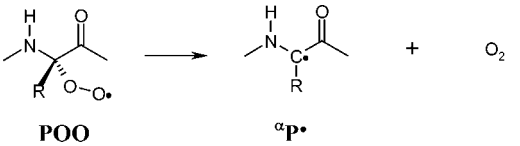

(1)

The corresponding isodesmic reaction is represented by process 2:

$$^{\alpha}\mathrm{P}^{\cdot}(\mathrm{res}) + \mathrm{POO(Gly)} \rightarrow \mathrm{POO(res)} + {}^{\alpha}\mathrm{P}^{\cdot}(\mathrm{Gly}) \quad (2)$$

The heat of reaction (2), $\Delta H^{\circ}(2)$, was evaluated from the energies obtained in the *ab initio* calculations at the B3LYP/6–31G(d) level. The BDE, $D_{\alpha\mathrm{CO}}(\mathrm{POO})$, is then given by

$$D_{\alpha\mathrm{CO}}[\mathrm{POO(res)}] = D_{\alpha\mathrm{CO}}[\mathrm{POO(Gly)}] - \Delta H^{\circ}(2) \quad (3)$$

In the present work, glycine [A(Gly)]- and glycylpeptide [P(Gly)]-derived species whose energies were derived at the CBS-RAD level were used as the reference molecules for free alanine amino acid and model alanine peptides, respectively.

The BDEs associated with removal of hydrogen, hydroxyl and hydroperoxy radicals, D_{OH}, D_{OO} and D^{α}_{CO}, respectively, were derived in an analogous manner.

Stereochemical considerations

Glycyl and alaninyl radicals, $^{\alpha}\mathrm{A}^{\cdot}$(Gly) and $^{\alpha}\mathrm{A}^{\cdot}$(Ala), and their peptide analogues, $^{\alpha}\mathrm{P}^{\cdot}$(Gly) and $^{\alpha}\mathrm{P}^{\cdot}$(Ala), are planar and may add O_2 from either side with equal probability to yield racemic peroxy products. In the case of $^{\alpha}\mathrm{P}^{\cdot}$, this is largely true even when the residue is part of an extended peptide chain in random-coil conformation since the nearest chiral centers of adjacent residues are separated from the radical site by a quasi-planar amide link. However, incorporation of the chain into β-sheet or α-helical secondary structure introduces an element of asymmetry to the $^{\alpha}$C site of interest and the diastereomeric derivatives may be of different energy and structure. In the present paper, we examine only the consequences of β-sheet secondary structure since the extreme deformation from planarity introduced by α-helical structure was previously shown to lead to considerable destabilization of $^{\alpha}$C-centered radicals.[14]

RESULTS AND DISCUSSION

Structures: AOOH (Gly), AOO(Gly), AOOH(Ala) and AOO (Ala)

The optimized local minimum energy structures of the glycine- and alanine-derived hydroperoxides, AOOH, and peroxy radicals, AOO, optimized at the B3LYP/6–31G(d) level are presented in Plate 1. Only the three most stable conformations, labeled **a**, **b** and **c**, of each species are shown. The electronic energies and vibrational ZPEs calculated at the B3LYP/6–31G(d) level are listed in Table S1 in the Supplementary material. The calculated values of $H^{\circ}_{298} - H^{\circ}_{0}$ and S°_{298} are also given there. Bond distances between heavy atoms, important hydrogen-bonding distances and the Ramachandran angles Φ and Ψ are given for each conformer in Plate 1. Full details of the structures are available from Table S2 of the Supplementary material.

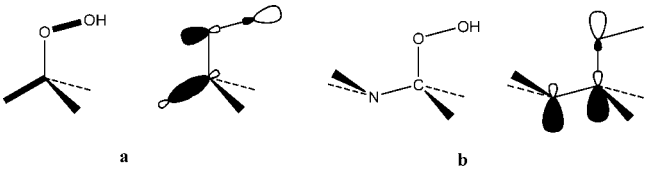

Figure 1. Stabilizing donor–acceptor interactions in hydroperoxides and peroxy radicals (not shown): (a) σ_{CX}–$\sigma_{\mathrm{OO}}{}^{*}$; (b) n_{N}–$\sigma_{\mathrm{CO}}{}^{*}$

The relative energies and structures in Plate 1 reflect a complex interplay of intramolecular interactions. In the more stable **a** and **b** conformations of AOOH(Gly) and AOOH(Ala), an intramolecular H bond to the acyl O atom is present. Each conformer also has an additional stabilizing element, the presence of a n_{N}-σ_{CO}* interaction [Fig. 1(b)]. Evidence for this is seen from the orientation of the amino group which places the n_{N} lone pair orbital in the favorable anti-coplanar arrangement with the $^{\alpha}$C—O bond. In the least stable conformation **c** of the AOOH species, the H-bond is to the free amino group and the n_{N}–σ_{CO}* interaction is absent. An additional stereoelectronic element that differentiates the **a** and **b** conformers is the donor–acceptor interaction between the antibonding orbital, σ_{OO}*, and the σ-bond which is anti-coplanar to it [Fig. 1(a)]. Judging from the relative energies of the **a** and **b** conformers shown in Plate 1, the donor ability of the σ-bonds is in the order σ_{CH} (or σ_{CMe}) $> \sigma_{\mathrm{CN}}$. Structures **b** with the $^{\alpha}$C—N bond anti-coplanar to the O—O bond are $\sim$5 kJ mol^{-1} less stable than structures **a** that have the $^{\alpha}$C—H (or $^{\alpha}$C—Me) bond in this position.

The stereoelectronic features of the peroxy radicals, AOO(Gly) and AOO(Ala), are slightly different from those of the parent hydroperoxides. The possibility of an H-bond is absent and each conformer has the n_{N}–σ_{CO}* interaction as seen from the orientation of the free amino group relative to the $^{\alpha}$C—O bond. The much longer $^{\alpha}$C—O bond [e.g. about 1.56 Å compared with 1.43 Å in AOOH(Gly)] lowers the σ_{CO}* orbitals and increases the importance of this interaction. Conformers **a** and **b** have almost the same energy.

Structures: POOH(Gly), POOH(Ala), POO(Gly) and POO(Ala)

The most stable conformers of the peroxy and hydroperoxy peptide derivatives of glycine and alanine are shown in Plate 2. These serve as models for residues in proteins. The backbones of all of the dipeptides are in the extended conformation ($\Phi \approx 180^{\circ}$, $\Psi \approx 180^{\circ}$) as would be expected in the random coil or β-sheet secondary structure. The energy differences between the three rotamers of the POOH species are substantially higher than was

the case for the AOOH species (Plate 1). The two lower energy conformers, **a** and **b**, have an intramolecular hydrogen bond with the oxygen atom of the formyl group (corresponding to the $i-1$ residue in a protein). In the most stable form, **a**, the O—O bond is almost eclipsed to the C—H (or C—Me) bond. The second lowest energy conformer, **b**, has the O—O bond positioned opposite the bond to the side-chain H (or Me). In this orientation, the σ–σ_{OO}* interaction [Fig. 1(a)] is maximized. The energy difference between the **a** and **b** conformers of POOH(Ala) is about 9 kJ mol^{-1} less than the difference in POOH(Gly). There are two possible explanations: the $^{\alpha}$C—Me bond may be a better donor than the $^{\alpha}$C—H bond, thus strengthening the σ–σ* interaction, and/or there is destabilization of the **a** conformer of POOH(Ala) by steric hindrance of the methyl group.

The preferred orientation of the O—O bond in the peroxy radicals, POO(Gly) and POO(Ala) (Plate 2) is opposite the C—N bond. This places the terminal O atom (the formal radical site) in close proximity to the H atom of the NH bond (of the amide group of the $i+1$ residue of a protein). This structure benefits either from a weak but stabilizing one-electron interaction between the singly occupied orbital of the radical site and σ_{NH}* or a normal H-bond, O···H—N, or both. Thus, the second conformer is 7–10 kJ mol^{-1} less stable than the first. The third conformer, in which a destabilizing three- or four-electron O···O interaction is present, is 5 kJ mol^{-1} less stable in the case of POO(Gly) and is 10 kJ mol^{-1} less stable in the case of POO(Ala).

Structures: alkoxy radicals, AO(Gly), AO(Ala), PO(Gly) and PO(Ala)

The minimum energy conformers of all of the alkoxy radical species are collected in Plate 3. In the case of the oxy radicals of the amino acids, AO(Gly) and AO(Ala), the $^{\alpha}$C—O bond is shorter by 0.07 Å than in the parent AOOH. In the peptide models, PO(Gly) and PO(Ala), this bond is 0.04 Å shorter still, indicating a distortion along the pathway to β-elimination of one of the groups attached to $^{\alpha}$C. The severe stretching of the $^{\alpha}$C—C bond (by 0.06–0.1 Å) suggests that it is this bond that is the most likely candidate for β-scission. This process is examined further below.

C—O BDEs of peroxy radicals: ROO (alkylperoxy), AOO(Gly), AOO(Ala), POO(Gly) and POO(Ala)

At the present level of theory, O_2 addition to $^{\alpha}$C-centered radicals (step 2 of Scheme 1) occurs without activation, as noted previously in the case of O_2+ethyl radical.[21] The enthalpy change for the reverse (step −2 of Scheme 1) is the $^{\alpha}$C—O BDE. There are no experimental determinations of C—O BDEs of AOO or POO, but values exist for simple alkyl peroxy radicals (ROO) both from experiment[22,23] and from other high-level calculations (Table 1).[24]

The CBS-RAD results (Table 1) are in almost perfect agreement with the high-level calculations of Brinck *et al.*,[24] and with the experimental values except for α-hydroxymethylperoxy radical, $HOCH_2OO^{\cdot}$. It had been concluded previously on the basis of theory that the experimental value for $HOCH_2OO^{\cdot}$ is probably incorrect.[24] The B3LYP calculations, whether with small [6–31G(d)] or large [6–311+G(3df,2p)] sets, yielded values which are 6–28 kJ mol^{-1} too low, with the discrepancy increasing with the complexity of the alkyl group. Single point calculations with the large basis set on small basis set structures give nearly the same energies as those obtained after full optimization with the large basis set. Therefore, in subsequent calculations for the peptide

Table 1. C—O bond dissociation enthalpies at 298 K (kJ mol^{-1})

Compound	SB//SB[a]	LB//LB[b]	LB//SB[c]	CBS-RAD	Other high-level calculations	Exp.
CH_3OO	131.2	124.9	124.7	137.0	148.1[d],136.4[e]	136.8 ± 3.8[f],134.7 ± 6.3[g]
CH_3CH_2OO	133.8	127.6	127.6	147.4		148.5 ± 8.4[f]
$(CH_3)_2CHOO$	135.0	127.9	128.3	157.7		155.2 ± 9.6[f]
$(CH_3)_3COO$	131.2	124.3	124.7	161.8		152.7 ± 7.5[f],126.3 ± 4.6[g]
$OHCH_2OO$	143.5	131.6	132.2	151.9	153.1[e]	68.2 ± 1.3[g]
CH_2CHCH_2OO	63.5	57.5	57.2	80.5		76.1 ± 2.1[g]
AOO(Gly)	49.4	35.8	35.7	69.9		—
AOO(Ala)	69.3[h]		69.4[h]	69.3[i]		—
POO(Gly)	65.4		52.7	88.7		—
POO(Ala)	85.8[j]		86.5[j]	85.8[i]		—

[a] SB//SB: 6–31G*//6–31G*.
[b] LB//SB: 6–311+1G (3df, 2p)//6–31G*.
[c] LB//LB: 6–311+G (3df, 2p)//6–311+G (3df,2p).
[d] G2 calculation from Ref. 24.
[e] CBS-Q calculation from Ref. 24.
[f] Ref. 23.
[g] Ref. 22.
[h] From isodesmic reaction using CBS-RAD value for AOO(Gly) as reference.
[i] Best estimated value.
[j] From isodesmic reaction using CBS-RAD value for POO(Gly) as reference.

model, we only perform single point calculation on the large basis set. From Table 1, it can be seen that for all of the species, the calculated results using the small basis were closer to experiment or high-level theory than with the large basis set. B3LYP/6–31G(d) optimized results underestimated the experimental values by 6–21 kJ mol^{-1}. The B3LYP/6–311+G(3df, 2p) procedure further underestimates the C—O BDE by 6–12 kJ mol^{-1}.

From Table 1, it can be seen that the alkylperoxy radicals, ROO, have the remarkable property that the C—O BDE increases as the stability of the product radical increases over the series R = CH_3, CH_3CH_2, $(CH_3)_2CH$. The trend is predicted to continue with R = $(CH_3)_3C$ at the highest theoretical level, CBS-RAD, but not at lower levels or by experiment. The anomalous behavior originates from stabilization of the parent ROO according to the ability of R to support a positive charge. It suggests that for these systems the ability to stabilize cation character in the parent by resonance structure **b** is more important than the stability of the radical product, i.e. resonance structure **c**. Thus the C—O BDE of $HOCH_2OO$ is predicted to be higher than that of CH_3OO, 153 vs 137 kJ mol^{-1}, respectively. A clear break occurs when R = A (a neutral amino acid) or P (the model peptide). The $^{\alpha}$C—O BDEs of AOO and POO are considerably lower, in the range 69–89 kJ mol^{-1}, indicating that these systems are less able to support a positive charge and that radical stability of the products determine the low $^{\alpha}$C—O BDEs.

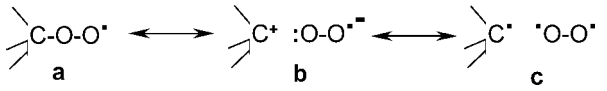

BDEs of hydroperoxides, ROOH, AOOH and POOH: O—H, O—O, C—O

O—H, O—O and C—O BDEs calculated at different levels of theory for CH_3OOH, AOOH(Gly), AOOH(Ala), POOH(Gly) and POOH(Ala) are listed in Table 2 together with experimental values for CH_3OOH[25] and high-level theoretical values for formylmethyl hydroperoxide ($OCHCH_2OOH$).[26] The latter compound has some rudimentary similarity to AOOH and POOH in that the site of OOH attachment is flanked by an acceptor group. The data in Table 2 permit one to assess the sensitivity of the various BDEs to the nature of the R group.

O—H BDEs. It can be seen from Table 2 that the CBS-RAD-calculated value of the O—H BDE of CH_3OOH is in good agreement with experiment and other high-level calculations. The B3LYP/6–31G(D) level underestimates the BDE by about 40 kJ mol^{-1}. At the B3LYP/6–311+G(3df, 2p) level, the O—H BDEs are underestimated by 20 kJ mol^{-1}. The OH BDE is almost the same for methyl and formylmethyl hydroperoxide, 365 kJ mol^{-1}. The CBS-RAD-derived O—H BDEs of AOOH(Gly) and POOH(Gly) are predicted to be higher by 10 and 20 kJ mol^{-1}, respectively, compared with methyl hydroperoxide. The increases are probably due to the presence of the H-bond in the parents (Plates 1 and 2). The O—H BDEs of AOOH(Ala) and POOH (Ala) were found to be essentially the same as the respective Gly values. The value of the O—H BDE in POOH(Gly) and POOH(Ala), about 380 kJ mol^{-1}, implies that the POO radical can be quenched by endogenous thiols such as cysteine or glutathione, S—H BDE = 370 kJ mol^{-1}.[27]

Table 2. BDE of hydroperoxides at 298 K (kJ mol^{-1})

Bond	Compound	SB//SB	LB//LB	LB//SB	CBS-RAD	Exp. or calculation values
O—H	CH_3	321.7	344.4	344.7	359.8	364.0 ± 4.2[a], 370.7 ± 2.5[b], 360.7[c], 358.2[d]
	AOOH(Gly)	331.5	348.3	348.5	370.5	365.2[e]
	AOOH(Ala)	367.9[f]		368.7[f]	368.7[g]	
	POOH(Gly)	348.3		365.4	380.3	
	POOH(Ala)	381.4[h]		382.8[h]	382.8[g]	
O—OH	CH_3	169.2	156.7	153.9	190.0	188.8[e]
	AOOH(Gly)	183.6	161.1	160.8	202.7	
	AOOH(Ala)	194.8[f]		195.9[f]	194.8[g]	
	POOH(Gly)	182.7		158.6	207.2	
	POOH(Ala)	207.9[h]		209.3[h]	207.9[g]	
C—OOH	CH_3	266.7	259.0	258.9	293.5	264.5[e]
	AOOH(Gly)	194.1	174.3	173.5	236.9	
	AOOH(Ala)	233.9[f]		234.8[f]	233.9[g]	
	POOH(Gly)	227.5		207.7	265.7	
	POOH(Ala)	263.9[h]		266.0[h]	263.9[g]	

[a] Ref. 25.
[b] Ref. 22.
[c] G2 calculation from Ref. 24.
[d] CBS-Q calculation from Ref. 24.
[e] From Ref. 26 for $OCHCH_2OOH$.
[f] From isodesmic reaction using CBS-RAD value for AOOH(Gly) as reference.
[g] Best estimated value.
[h] From isodesmic reaction using CBS-RAD value for POOH(Gly) as reference.

O—O BDEs. Although the O—O bond may be expected to be more sensitive to the nature of R, in fact high-level calculations indicate that this not the case.[26] The O—O BDE of both CH_3CH_2OOH and $OCHCH_2OOH$ is 189 kJ mol^{-1},[26] and the value for CH_3OOH is predicted to be 190 kJ mol^{-1} (Table 2). In the case of AOOH(Gly) and POOH(Gly), the O—O BDEs are higher by 13 and 17 kJ mol^{-1}, respectively. As noted above, the increase is largely attributable to the H-bond in the parent. In this case, as was noted with the peroxy radicals, the calculated results obtained with the small basis set are closer to the CBS-RAD value.

C—O BDEs. The C—O BDEs will be most sensitive to the nature of R, decreasing with increasing stability of the product C-centered radical. For the C—OOH BDEs, the order of the BDE is $CH_3OOH > OCHCH_2OOH >$ POOH(Gly) > POOH(Ala) > AOOH(Gly) > AOOH (Ala). Unlike the peroxy radical case, the order of C—O BDEs of the hydroperoxides follows strictly the order of stabilities of the product radicals. In this case also, calculated results obtained from the smaller 6–31G(d) basis set agree better with the CBS-RAD values than do those obtained with the larger 6–311+G(3df,2p) basis set.

Effect of β-sheet constraints on the BDEs of POO(Gly), POO(Ala), POOH(Gly) and POOH(Ala)

The BDEs of the $^{\alpha}$C—O, O—O and O—H bonds of the peptide model peroxy radicals and hydroperoxides are collected in Table 3, where the effects of β-sheet secondary structure are examined. β-Sheet secondary structure was modeled by constraining the Ramachandran Φ and Ψ angles to −150 and 150°, respectively, in both the parent species and the product radicals. For comparison, the BDEs of the fully optimized Gly structures are repeated from Tables 1 and 2. The BDEs for β-sheet-constrained Gly-derived and all Ala-derived species were obtained by isodesmic correction using the optimized Gly values as reference.

Introduction of an OO or OOH group to the $^{\alpha}$C-site of Gly renders it a chiral center. Attachment at the pro-*S* site corresponds to the normal position of the side chain in L-amino acids. Thus (*S*)-POO(Ala) and (*S*)-POOH(Ala) have the methyl group oriented as in D-alanine, whereas the *R*-enantiomers have the methyl oriented in the natural position. An important consequence of constraining the Ramachandran angles Φ and Ψ to model β-sheet secondary structure is to introduce an additional element of stereochemistry, rendering the *R*- and *S*-stereoisomers diastereomeric. The β-sheet-constrained (*S*)- and (*R*)-Gly derivatives are shown in Plate 4. The pleated structure originates from the need to accommodate the bulkier side-chain in the less hindered out-of-plane orientation. The OO group has about the same steric bulk as a methyl group, as can be seen from the near-planar backbone geometry of optimized (*R*)-POO(Ala), Φ = 176°, Ψ = 176° (Table 3). The possibility of forming strong H-bonds in the case of POOH brings in additional considerations (see below).

POO(Gly) and POO(Ala). As discussed in the section on BDEs, homolysis of the $^{\alpha}$C—O bond requires 89 kJ mol^{-1} and yields the $^{\alpha}$P$^{\cdot}$(Gly) radical, whose optimized structure is planar.[20] The β-sheet distorted structure is 17 kJ mol^{-1} higher in energy owing to partial loss of captodative stabilization. In the case of (*S*)-POO(Gly) (β-sheet), $D_{\alpha CO}$ is higher than the optimized value by 10 kJ mol^{-1}, indicating that the constrained geometry is higher in energy than the optimized geometry of (*S*)-POO(Gly) by only 7 kJ mol^{-1}. On the other hand, the (*R*)-POO(Gly) β-sheet structure has $D_{\alpha CO}$ lower by 10 kJ mol^{-1}, indicating that it is destabilized by 27 kJ mol^{-1} relative to the optimized structure which has the Ramachandran angles reversed in sign (Table 3).

$D_{\alpha CO}$ of the optimized structures is almost the same for POO(Gly) and POO(Ala), i.e. there is little effect on BDE

Table 3. Effect of β-sheet structure on the BDEs[a] of POO and POOH 298 K (kJ mol^{-1})

			POO	POOH		
Compound	Φ	Ψ	C—O	COO—H	O—OH	C—OOH
(*R*)-Gly–opt[b,c]	154	−176[d]	88.7	380.3	207.2	265.7
	−174	161[e]				
(*S*)-Gly–β-sheet[f]	−150	150	98.7	362.1	194.8	257.5
(*R*)-Gly–β-sheet[f]	−150	150	77.6	404.1	217.0	278.4
(*R*)-Ala–opt[c]	176	176[d]	85.8	381.4	207.9	263.9
	−162	155[e]				
(*S*)-Ala–β-sheet	−150	150	88.3	354.7	191.9	239.7
(*R*)-Ala–β-sheet	−150	150	83.3	390.3	204.0	270.3

[a] By isodesmic correction based on Gly–opt values.
[b] Directly from CBS-RAD energies.
[c] See Plate 2 for structures.
[d] POO values.
[e] POOH values.
[f] See Plate 4 for structures.

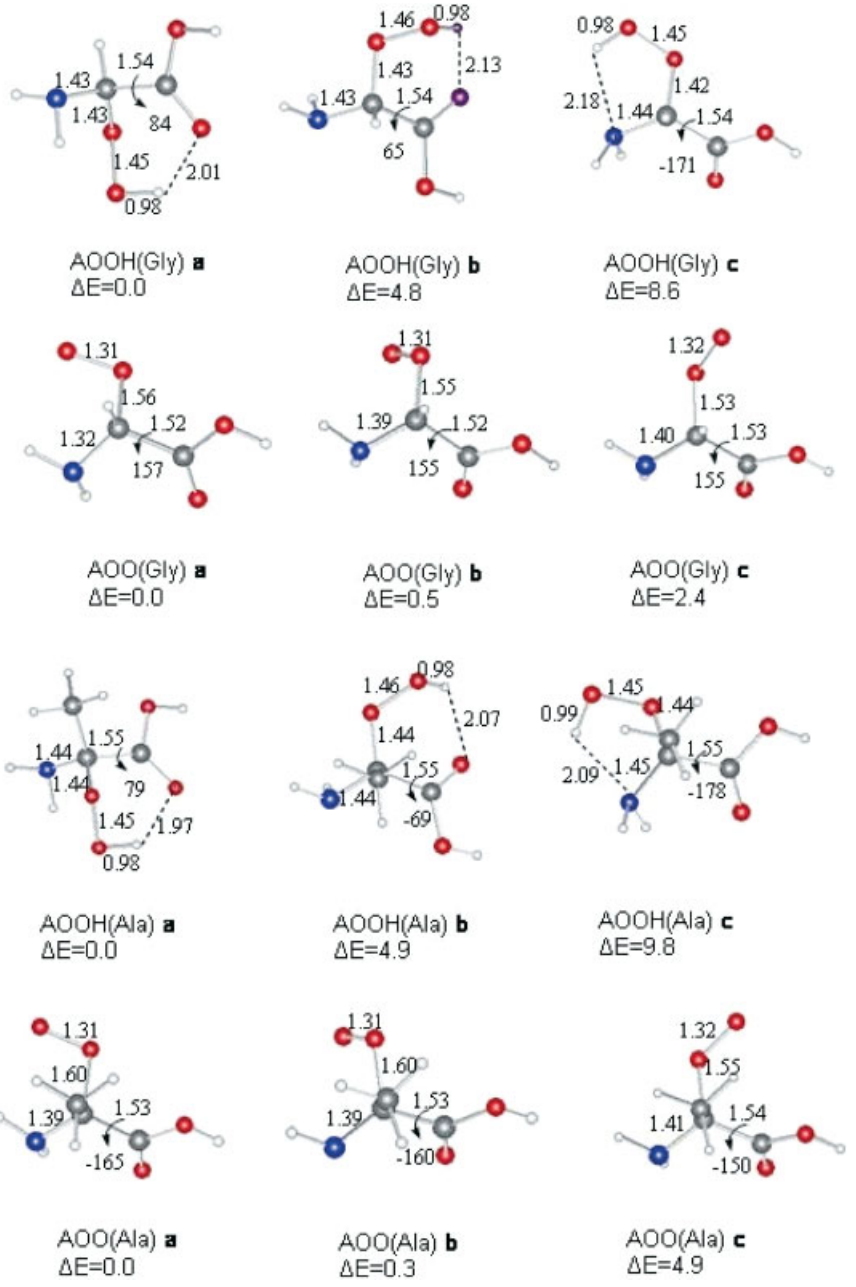

Plate 1. Different orientations of the amino acid peroxyl species with respect to rotation of the CO bond in *R*-isomers of AOO and AOOH: ΔE in kJ mol^{-1}, bond lengths in Å, angles in degrees

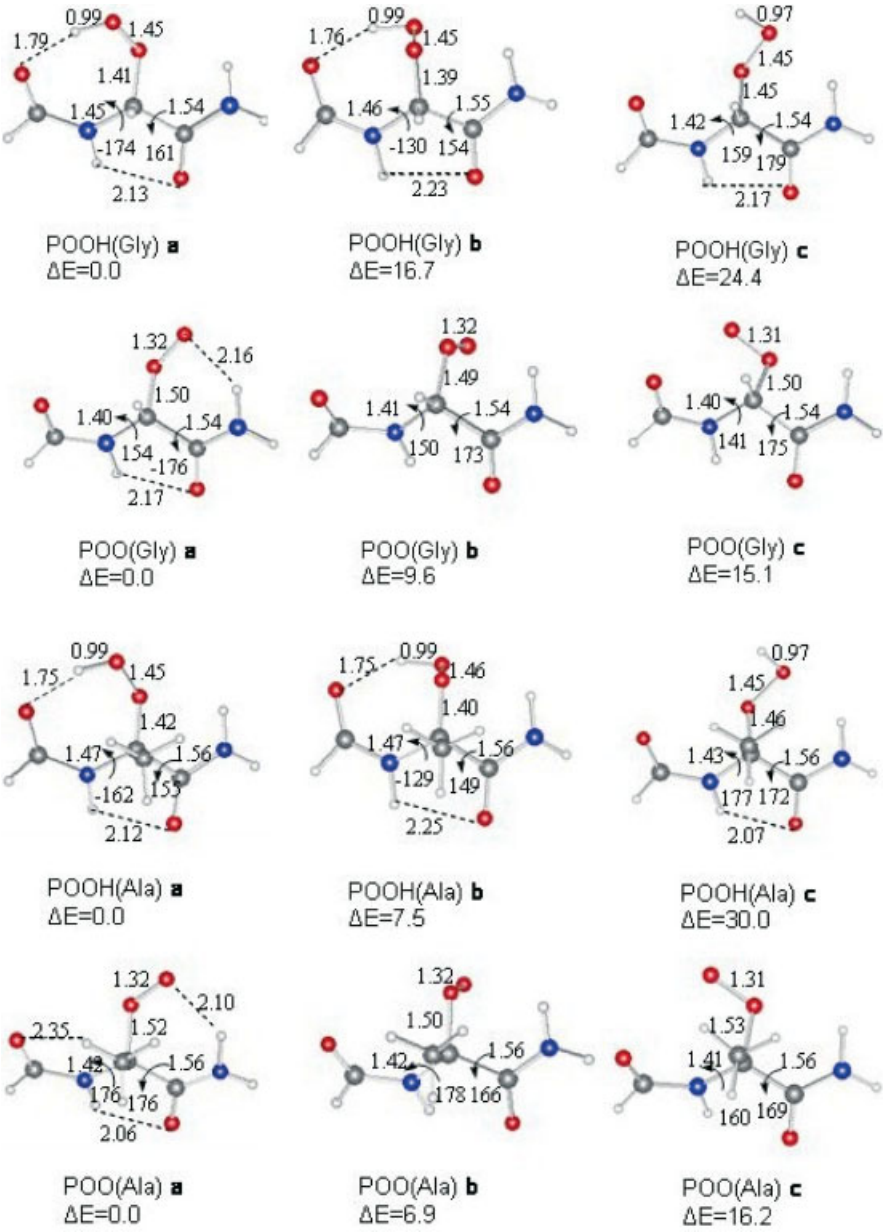

Plate 2. Different orientations of the peroxide with respect to rotation of the CO bond in *R*-isomers of POO and POOH: ΔE in kJ mol^{-1}, bond lengths in Å, angles in degrees

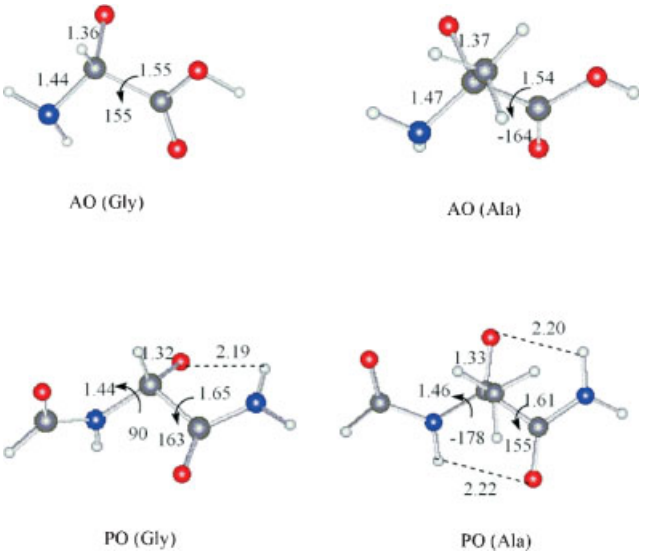

Plate 3. B3LYP/6–31G (d) optimized structures of the *R*-isomers of AO and PO. In AO, the torsion angle refers to N—$^{\alpha}$C—C—O(H); in PO, the torsion angles are the Ramachandran angles, $\Phi = $ C—N—$^{\alpha}$C—C, $\Psi = $ N—$^{\alpha}$C—C—N. Distances in Å, angles in degrees

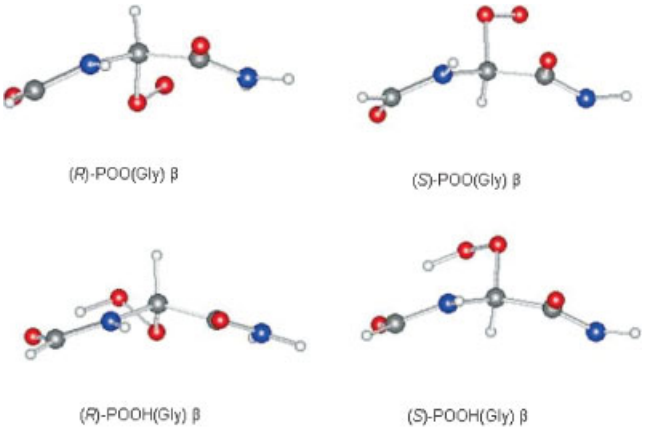

Plate 4. Structures of *S*- and *R*-stereoisomers of POO(Gly) in a β-sheet. Distances in Å, angles in degrees

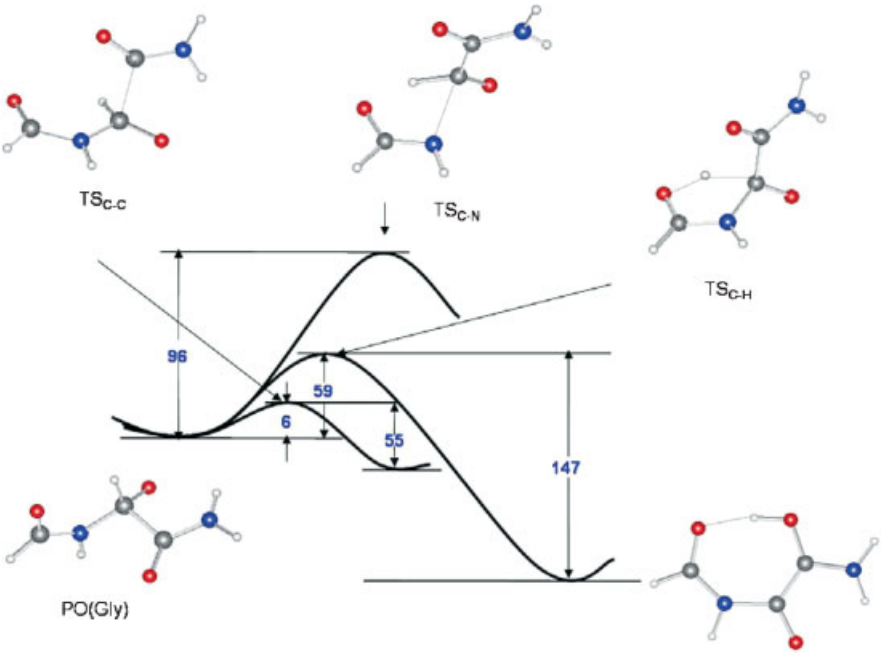

Plate 5. Free energy profile for β-scission reactions of PO(Gly). Energies in kJ mol^{-1}

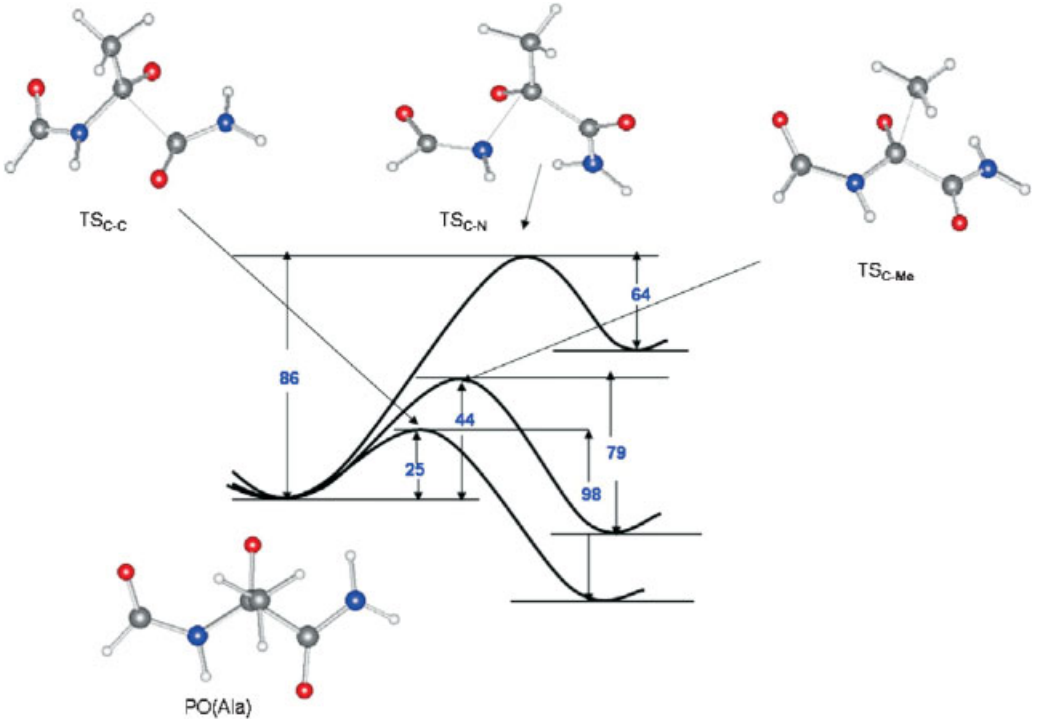

Plate 6. Free energy profile for β-scission reactions of PO(Ala). Energies in kJ mol^{-1}

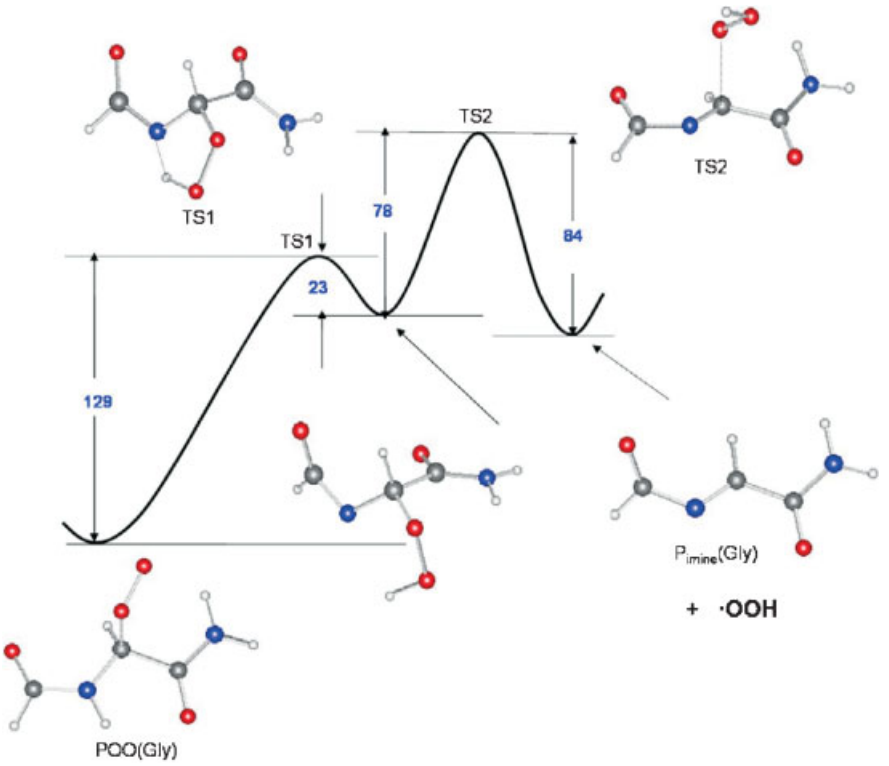

Plate 7. Free energy profile for OOH radical elimination reaction of POO(Gly). Energies in kJ mol^{-1}

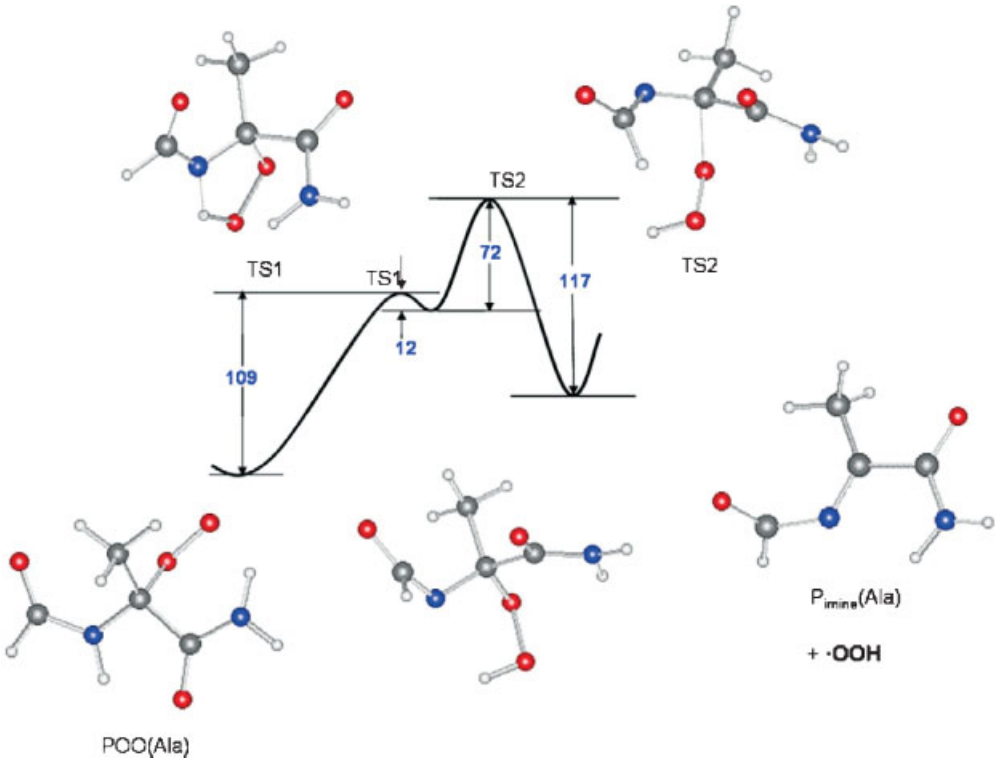

Plate 8. Free energy profile for OOH radical elimination reaction of POO(Ala). Energies in kJ mol^{-1}

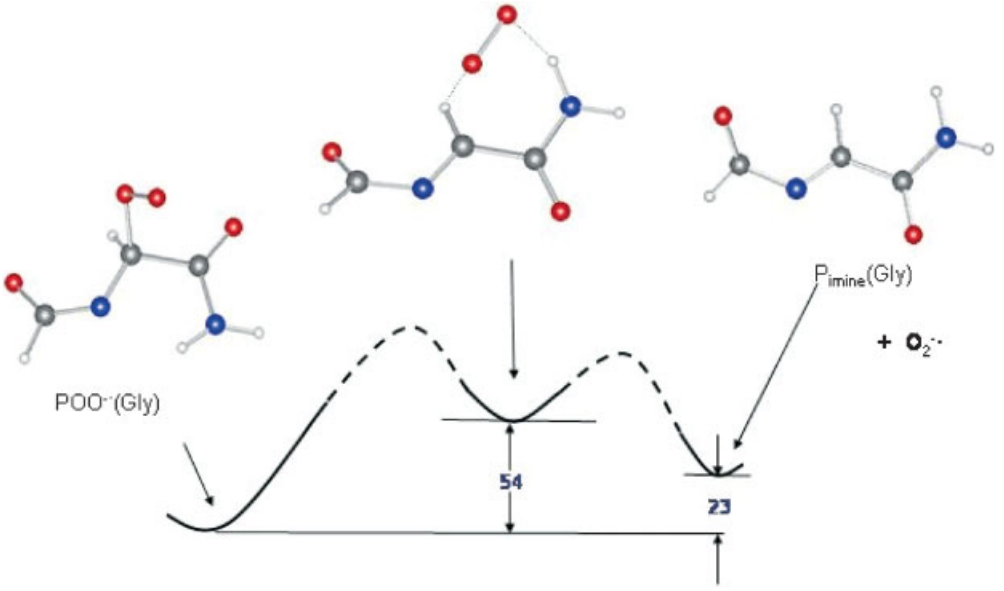

Plate 9. Partial free energy profile for base-catalyzed superoxide elimination reaction of POO(Gly). Energies in kJ mol^{-1}

when altering the side-chain from H to methyl group. The imposition of β-sheet constraints on the POO(Ala) stereoisomers has little effect on the $^{\alpha}$C—O BDE. The $D_{\alpha CO}$ of the (*S*)- and (*R*)-β-sheet structures differs by +3 and −3 kJ mol^{-1}, respectively, from the optimized value, 86 kJ mol^{-1}, owing to the similarity of the steric bulk of the OO and CH_3 groups.

POOH(Gly) and POOH(Ala). The imposition of β-sheet constraints has a more significant effect on O—H, O—O and $^{\alpha}$C—O BDEs of the POOH stereoisomers (Plate 4) than it did on the $^{\alpha}$C—O BDE of POO. This is largely due to the preference of the OOH group for the more hindered equatorial position because it permits the formation of a strong intramolecular H-bond to the carbonyl of the $i-1$ residue (the formyl group on the models). Hence the (R)-POOH β-sheet diastereomers have substantially lower energy than the *S*-diastereomers. Homolysis of any of the O—H, O—O or $^{\alpha}$C—O bonds results in the loss of the H-bond. Consequently, the BDEs of the *R*-isomers are higher than the BDEs of the *S*-isomers by 35–42, 12–22 and 21–30 kJ mol^{-1}, respectively, for the O—H, O—O and $^{\alpha}$C—O bonds.

Oxidative damage in β-sheet secondary structure. It should be noted that the above considerations apply fully only to a strand of a β-sheet that is on the edge of the sheet. The only residue on an interior strand of β-sheet secondary structure that can be damaged by H-abstraction from the $^{\alpha}$C-site is glycine.[28] On an interior strand, the equatorial site does not have room for a group larger than H and the $^{\alpha}$C—H bond is sterically protected from radical attack. Only glycine with a second $^{\alpha}$C—H bond in the exposed axial orientation can be oxidized by H abstraction. Thus, in practice, only (*S*)-POO(Gly) and (*S*)-POOH(Gly) would be expected to occur in this situation.

β-Scission reactions of PO(Gly) and PO(Ala)

Table 4. Enthalpies, entropies and free energies of activation for the β-scission of PO(Gly) and PO(Ala) at 298 K in the gas phase

Species	$\Delta H^{\ddagger}$ (kJ mol^{-1})	$\Delta S^{\ddagger}$ (J K^{-1} mol^{-1})	$\Delta G^{\ddagger}$ (kJ mol^{-1})
PO(Gly) $^{\alpha}$C···H	55.3	−13.1	59.2
PO(Gly) $^{\alpha}$C···$^{\text{carbonyl}}$C	4.7	−3.5	5.8
PO(Gly) $^{\alpha}$C···N	97.6	5.6	95.9
PO(Ala) $^{\alpha}$C···CH_3	45.8	6.8	43.8
PO(Ala) $^{\alpha}$C···$^{\text{carbonyl}}$C	21.8	−9.9	24.7
PO(Ala) $^{\alpha}$C·N	89.2	12.2	85.6

solutions of the cyclic anhydrides of glycine (cGG) and alanine (cAA).[3] The initially generated $^{\alpha}$C radicals react rapidly with oxygen to produce peroxy radicals, cGGOO and cAAOO. Under conditions of neutral pH, the product peroxy radicals undergo bimolecular reaction eliminating O_2 and yielding the analogous oxy radicals, cGGO and cAAO. Competitive with H-atom abstraction, the oxy radicals undergo β-scission reactions that result in degradation of the ring. cGGO and cAAO are not good models for the chemistry of PO(Gly) and PO(Ala) because the cyclic geometry considerably slows the β-scission process relative to the acyclic analogues.

We present here a qualitative analysis of the three β-scission pathways available to PO species at the B3LYP/6–31G(d) level of theory. Transition structures were located for each of the three pathways for PO(Gly) and PO(Ala), labeled TS_{CH} (or TS_{CMe}), TS_{CN} and TS_{CC}, for cleavage of the $^{\alpha}$C—H (or $^{\alpha}$C—Me), $^{\alpha}$C—N and $^{\alpha}$C—$^{\text{carbonyl}}$C bonds, respectively. The gas-phase enthalpies, entropies and free energies of activation at 298 K are collected in Table 4. The free energy profiles and structures in the case of PO(Gly) and PO(Ala) are plotted in Plates 5 and 6, respectively. Because the transition structures resemble the reactants and all species involved are neutral, the gas-phase data in Table 4 should yield a qualitatively correct picture in the aqueous phase.

In the case of PO(Gly), the $^{\alpha}$C—$^{\text{carbonyl}}$C cleavage has the lowest energy barrier, only 6 kJ mol^{-1}. Similarly,

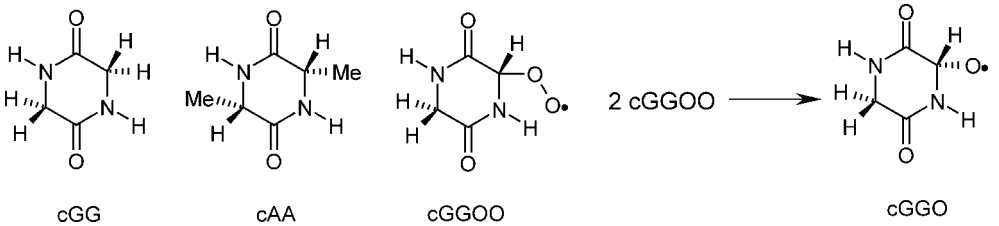

Alkoxy radicals undergo β-cleavage to yield carbonyl compounds and daughter radicals. An example is shown as step 10 of Scheme 1. The activation energy for the process depends in large part on the stability of the daughter radicals.[29] The reactions of peptide oxy radicals of the type PO have been studied by radiolysis of aqueous

cleavage of the $^{\alpha}$C—$^{\text{carbonyl}}$C bond of PO(Ala) is hindered by only 25 kJ mol^{-1}. A previous study found that activation enthalpies calculated at the B3LYP/6–31G(d) level tend to be *higher* than CBS-RAD values (by 6–13 kJ mol^{-1} in the case of simple alkoxy radicals).[29] This is unlikely to be the case here in view of the

overestimation of the stability of the radical products (cf. the $^{\alpha}$C—O BDE data for AOOH and POOH in Table 2). In any case, the data suggest that the backbone $^{\alpha}$C—$^{\text{carbonyl}}$C cleavage of peptide alkoxy radicals has a low barrier. The TS for $^{\alpha}$C—$^{\text{carbonyl}}$C cleavage, TS_{CC}, has almost a fully formed carbonyl double bond [1.26 Å for PO(Gly) and 1.24 Å for PO(Ala)] and a substantially broken $^{\alpha}$C—$^{\text{carbonyl}}$C bond [1.98 Å for PO(Gly) and 2.07 Å for PO(Ala)]. The radical product of this β-cleavage pathway for PO is the aminocarbonyl radical, $OC^{\cdot}NH_2$, which in a polypeptide would correspond to an N-terminal aminocarbonyl radical.

β-Scission of the $^{\alpha}$C—H (Gly) and $^{\alpha}$C—Me (Ala) bonds is hindered by modest barriers, 59 kJ mol^{-1} (Plate 5) and 44 kJ mol^{-1} (Plate 6), respectively. In the case of PO(Ala), the radical product of β-scission is methyl radical, as expected. However, the equivalent reaction in the case of PO(Gly) follows a different course. TS_H corresponds to intramolecular transfer of the H from $^{\alpha}$C to the oxygen atom of the formyl group (corresponding to the $i-1$ residue). The intrinsic reaction coordinate (IRC) for this process indicates that the putative product radical, R1 (not shown in Plate 5), is not a stationary point. Rather, subsequent rotation about the $^{\alpha}$C—N bond leads to a second intramolecular transfer of the H atom to the other amide oxygen atom, to yield radical R2 (Plate 5) without activation. The free energy change for the reaction PO(Gly) → R2 is −88 kJ mol^{-1}. The exceptional stability of R2, which is planar, originates in captodative stabilization by two donor groups, OH and NH_2, and an acceptor group, the carbonyl group at the oxidized $^{\alpha}$C-site, as well as the intramolecular H bond.

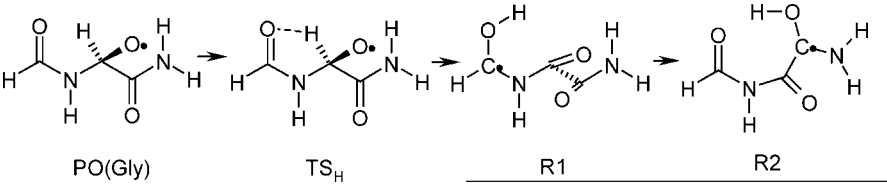

β-Scission of the $^{\alpha}$C—N bond has the highest activation, 96 and 86 kJ mol^{-1} for PO(Gly) and PO(Ala), respectively. The transition structures, TS_{CN}, are shown in Plates 5 and 6, respectively. The total reaction enthalpy of $^{\alpha}$C···N cleavage β-scission for PO(Gly) calculated at the CBS-RAD level is 89 kJ mol^{-1}, indicating that this process is highly endothermic. This pathway was not pursued further.

Reactions of the peroxy radical: POO(Gly) and POO(Ala)

The central radicals of the present study are the peroxy radicals of glycyl residues, modeled by POO(Gly), and most other residues, modeled by POO(Ala). The reactions are shown in Scheme 1. Homolytic rupture of the $^{\alpha}$C—O bond (step −2) was discussed above. It proceeds endothermically to $O_2+^{\alpha}P^{\cdot}$ radical with no intervening barrier. Therefore, the enthalpy of activation for step −2 is the $^{\alpha}$C—O BDE, 88.7 and 85.8 kJ mol^{-1} for the Gly and Ala derivatives, respectively. These values are appropriate for the gaseous phase, but probably would not be very different in solution. The reactions of peroxy radicals, including cGGOO and cAAOO [the cyclic analogues of POO(Gly) and POO(Ala)], in aqueous solution have been reviewed.[2,10,11] Under neutral conditions, slow elimination of $HOO^{\cdot}$ is observed (step 4). Under alkaline conditions, rapid evolution of superoxide anion radical occurs (step 5). In either case, hydrolysis of the coproduct imine takes place with consequent cleavage of the backbone (step 7). We consider separately below the possible routes for unimolecular decay of POO(Gly) and POO(Ala) under neutral conditions and under alkaline conditions.

Neutral pH (Scheme 1, step 4). The reaction kinetics of peroxy radicals of cGG and cAA have been studied by pulse radiolysis of aqueous solutions,[12] but there are no reported similar studies on linear peptides. Under neutral conditions, in the case of α-hydroxy peroxy radicals, it was concluded by Bothe *et al.*[13] that the concerted elimination of $HOO^{\cdot}$ could occur via an intramolecular

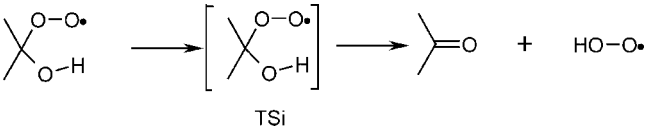

cyclic five-membered transition state, TSi. The analogous process, cGGOO → TSi_{cGGOO} → cGG_{imine}, was not observed.[12] We have examined this process in our acyclic POO(Gly) and POO(Ala) models. The reaction in each case proceeds in two steps, for which the calculated enthalpies, entropies, and free energies of activation are collected in Table 5. Again we assume that because no ionic species are involved the gas-phase data are qualitatively applicable to aqueous solution.

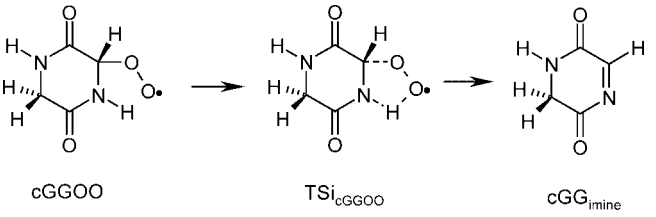

Table 5. Enthalpies, entropies and free energies of activation for POO → P_{imine}+HOO· at 298 K in the gas phase

Species	$\Delta H^{\ddagger}$ (kJ mol^{-1})	$\Delta S^{\ddagger}$ (J K^{-1} mol^{-1})	$\Delta G^{\ddagger}$ (kJ mol^{-1})
POO(Gly) → Int(Gly)[a]	129.6	3.4	128.6
Int(Gly) → P_{imine}(Gly) +HOO·	80.7	8.3	78.2
POO(Ala) → Int(Ala)[b]	109.9	1.8	109.4
Int(Ala) → P_{imine}(Ala) +HOO·	73.5	6.7	71.6

[a] Int(Gly) is the intermediate shown in Plate 7.
[b] Int(Ala) is the intermediate shown in Plate 8.

In POO(Gly) (Plate 7), the first transition structure, at +129 kJ mol^{-1}, corresponds to the intramolecular H atom transfer from the amide N atom to the terminal O of the peroxy radical site. Subsequent IRC analysis gave rise to an intermediate 23 kJ mol^{-1} lower than TS1, in which the HOO group was still attached to the $^{\alpha}$C-site. This N-radical intermediate then proceeds through a second transition state, 78 kJ mol^{-1} higher than the intermediate, to give the acyl imine product. The overall B3LYP/6–31G(d) barrier for the non-concerted elimination of HOO from POO(Gly) is 184 kJ mol^{-1}, and the free energy change for the reaction at this level is 100 kJ mol^{-1}. A more accurate estimate for the reaction free energy, 99 kJ mol^{-1}, is obtained by CBS-RAD calculation. Analogous analysis was applied to POO(Ala). Reaction route analysis (shown in Plate 8) shows that POO(Ala) also undergoes HOO· elimination in a non-concerted process. The reaction free energy for POO(Ala) → P_{imine}(Ala)+HOO· is predicted to be +61 kJ mol^{-1} at the CBS-RAD level [+52 kJ mol^{-1} at the B3LYP/6–31G(d) level].

Neutral pH (Scheme 1, step 5). We examine the possibility that POO may fragment by heterolysis to yield superoxide and the protonated imine, $P_{imine}H^+$, in the first step. CBS-RAD calculation of the reaction enthalpy for POO(Gly) → $P_{imine}H^+$+$O_2^{-\cdot}$ in the gaseous phase is 755 kJ mol^{-1}, which corresponds to a free energy change of 716 kJ mol^{-1}. Solvent stabilization of the resulting ions was estimated by COSMO at the B3LYP/6–31+G(d) level and using cavities defined by the 0.001 isodensity surfaces of the species involved: POO(Gly), $\Delta G_{solv} = -43.3$ kJ mol^{-1}; $P_{imine}H^+$, $\Delta G_{solv} = -307.5$ kJ mol^{-1}; $O_2^{-\cdot}$, $\Delta G_{solv} = -309.3$ kJ mol^{-1}. Thus, after inclusion of the solvation, the predicted free energy change for the heterolysis reaction in water is predicted to be 142.8 kJ mol^{-1}. Since the pK_a of $O_2^{-\cdot}$ is about 4.8,[30] an additional stabilization of about 27 kJ mol^{-1} is obtained by protonation of the anion to form HOO at neutral pH. Thus, the free energy change for reaction (4) is about 115 kJ mol^{-1}.

$$\mathrm{POO(Gly)} + \mathrm{H^+(aq)} \rightarrow \mathrm{P_{imine}H^+(Gly)} + \mathrm{HOO^{\cdot}} \quad (4)$$

This is to be compared with the free energy of homolytic rupture of the $^{\alpha}$C—O bond, which is about 48 kJ mol^{-1} (estimated from the CBS-RAD enthalpy change, 89 kJ mol^{-1} for loss of O_2).

Alkaline pH (Scheme 1, step 6). Under alkaline conditions, decomposition of cGGOO and cAAOO occurs rapidly in two steps: base-catalyzed deprotonation of the amide group to give an intermediate anion, e.g. cGGOO$^-$, which rapidly loses $O_2^{-\cdot}$. We examined this process in POO [Eqn (5)]. A partial free energy profile is shown in Plate 9.

$$\mathrm{POO^-(Gly)} \rightarrow \mathrm{P_{imine}(Gly)} + \mathrm{O_2^{-\cdot}} \quad (5)$$

The base-catalyzed loss of superoxide is predicted to involve an intermediate (Plate 9) in which the $^{\alpha}$C—O bond is broken but the $O_2^{-\cdot}$ anion remains H-bonded to the NH of the amide (of the i+1 residue). The free energy change for reaction (5) in the gas phase is 201 kJ mol^{-1}, as derived from the CBS-RAD enthalpy change. The COSMO-derived free energies of aqueous solvation for the species involved are POO$^-$(Gly), $\Delta G_{solv} = -214.6$ kJ mol^{-1}; P_{imine}(Gly), $\Delta G_{solv} = -44.4$ kJ mol^{-1}; $O_2^{-\cdot}$, $\Delta G_{solv} = -309.2$ kJ mol^{-1}. Thus the overall free energy of reaction (5) in water is predicted to be 23 kJ mol^{-1} (Plate 9).

CONCLUSIONS

Ab initio computations were used to investigate the structures of oxygen adducts to the $^{\alpha}$C-site of glycine and alanine, both as free neutral amino acids and as residues in model peptides (intended to mimic the environment in proteins). The $^{\alpha}$C-substituted peroxy radicals of both peptide model residues, POO, have $^{\alpha}$C—O bond dissociation enthalpies (BDEs) that are < 90 kJ mol^{-1}, substantially lower than for alkyl peroxy radicals, ROO (Table 1). Oxygen addition to the $^{\alpha}$C-site takes place without an intervening barrier. The O—H BDEs of the corresponding hydroperoxides, POOH, are $\sim$380 kJ mol^{-1}, indicating that the POO radical is quenchable by thiols such as cysteine or glutahione. The O—O BDEs of POOH are $\sim$208 kJ mol^{-1} and the $^{\alpha}$C—O BDEs are $\sim$265 kJ mol^{-1}. Variation in any of the parameters in the optimized structures are less than $\pm$5 kJ mol^{-1}, which suggests that none of the POO or POOH bonds are sensitive to the nature of the residue in the unstructured environment of a random coil. The effect of the more restricted peptide environment of β-sheet secondary structure on the BDEs was estimated by constraining the Ramachandran dihedral angles, Φ and Ψ, to values typical of β-sheets. In glycyl residues, the preferred stereochemistry at the $^{\alpha}$C-site of peroxy radical is *S*. On edge strands, the OOH group prefers to occupy the equatorial pro-*R* site in which it can form a strong intramolecular H-bond.

Various reactions of the peroxy radicals, POO, were investigated. Besides the quenching reaction, the least hindered process is homolysis of the $^{\alpha}$C—O bond, namely the reverse of the O_2 addition reaction to $^{\alpha}$C-centered radicals, for which the free energy change is calculated to be about $+48\,kJ\,mol^{-1}$ in POO(Gly). Heterolysis to give superoxide in water under conditions of neutral pH is predicted to be endothermic by about $115\,kJ\,mol^{-1}$. Under alkaline conditions, loss of superoxide is predicted to be endothermic by $23\,kJ\,mol^{-1}$.

Supplementary material

A table containing the primary data (electronic energy, zero point energy, H°_{298}–H°_{0} and entropy at 298 K) of each species discussed in the text and a table containing the Cartesian coordinates of each species are available in Wiley Interscience.

Acknowledgements

We are grateful to the Natural Sciences and Engineering Council of Canada (NSERC) for financial support of this work. We are also indebted to Patrick Brunelle for assistance with the computations.

REFERENCES

1. Stadman ER. *Annu. Rev. Biochem*. 1993; **62**: 797–821.
2. Hawkins CL, Davies MJ. *Biochim. Biophys. Acta Bioenerg*. 2001; **1504**: 196–219.
3. Von Sonntag C. *The Chemical Basis of Radiation Biology*. Taylor and Francis: London, 1987
4. Davies KJA (ed). *Oxidative Damage and Repair: Chemical, Biological and Medical Aspects*. Pergamon Press: New York, 1991.
5. Cheeseman KH. In *Immunopharmacology of Free Radical Species*, Blake D, Winyard PG (eds). Academic Press: New York, 1995.
6. Markesbery WR, Carney JM. *Brain Pathol.* 1999; **9**: 133–146.
7. Smith MA, Sayre LM, Monnier VM, Perry G. *Trends Neurosci.* 1995; **18**: 172–176.
8. Smith MA, Perry G, Richey PL, Sayre LM, Anderson VE, Beal MF, Kowall N. *Nature (London)* 1996; **382**: 120–121.
9. Garrison WM. *Chem. Rev.* 1987; **87**: 381–398.
10. Von Sonntag C, Schuchmann H-P. In *Peroxyl Radicals*, Alfassi ZB (ed). Wiley: New York, 1997.
11. Mieden OJ, von Sonntag C. *J. Chem. Soc., Perkin Trans. 2* 1989; 2071–2078.
12. Mieden OJ, Schuchmann MN, von Sonntag C. *J. Phys. Chem.* 1993; **97**: 3783–3790.
13. Bothe E, Behrens G, Schulte-Frohlinde D. *Z. Naturforsch., Teil B* 1977; **32**: 886–889.
14. Rauk A, Yu D, Armstrong DA. *J. Am. Chem. Soc.* 1997; **119**: 208–217.
15. Davies MJ. *Arch. Biochem. Biophys*. 1996; **336**: 163–172.
16. Davies MJ, Fu S, Dean RT. *Biochem. J.* 1995; **305**: 643–649.
17. Frisch MJ, Trucks GW, Schlegel HB, Scuseria GE, Robb MA, Cheeseman JR, Zakrzewski VG, Montgomery JA Jr, Stratmann RE, Burant JC, Dapprich S, Millam JM, Daniels AD, Kudin KN, Strain MC, Farkas O, Tomasi J, Barone V, Cossi M, Cammi R, Mennucci B, Pomelli C, Adamo C, Clifford S, Ochterski J, Petersson GA, Ayala PY, Cui Q, Morokuma K, Malick DK, Rabuck AD, Raghavachari K, Foresman JB, Cioslowski J, Ortiz JV, Baboul AG, Stefanov BB, Liashenko A, Piskorz P, Komaromi I, Gomperts R, Martin LR, Fox DJ, Keith T, Al-Laham MA, Peng CY, Nanayakkara A, Gonzalez C, Challacombe M, Gill PMW, Johnson B, Chen W, Wong MW, Andres JL, Gonzalez C, Head-Gordon M, Replogle ES, Pople JA. *Gaussian 98, Revision A.7*. Gaussian: Pittsburgh, PA, 1998.
18. Mayer PM, Parkinson CJ, Smith DM, Radom L. *J. Chem. Phys.* 1998; **108**: 604–615.
19. Barone V, Cossi M. *J. Phys. Chem. A* 1998; **102**: 1995–2001.
20. Armstrong DA, Yu D, Rauk A. *Can. J. Chem.* 1996; **74**: 1192–1199.
21. Sheng CY, Bozzelli JW, Dean AM, Chang AY. *J. Phys. Chem. A* 2002; **106**: 7276–7293.
22. Benson SW. *J. Phys. Chem*. 1996; **100**: 13544–13547.
23. Knyazev VD, Slagle IR. *J. Phys. Chem. A* 1998; **102**: 1770–1778.
24. Brinck T, Lee HN, Jonsson M. *J. Phys. Chem. A* 1999; **103**: 7094–7104.
25. Clifford EP, Wenthold PG, Gareyev R, Lineberger WC, DePuy CH, Bierbaum VM, Ellison GB. *J. Chem. Phys.* 1998; **109**: 10293–10310.
26. Lee J, Bozzelli JW. *J. Phys. Chem. A* 2003; **107**: 3778–3791.
27. Armstrong DA, Yu D, Rauk A. *J. Am. Chem. Soc.* 1998; **120**: 8848–8855.
28. Rauk A, Armstrong DA. *J. Am. Chem. Soc.* 2000; **122**: 4185–4192.
29. Rauk A, Boyd RJ, Boyd S, Henry DJ, Radom L. *Can. J. Chem.* 2003; **81**: 431–442, and references cited therein.
30. De Grey ADNJ. *DNA Cell Biol.* 2002; **21**: 251–257.